# Increased crystal porosity and enhanced gas adsorption by intracolumnar gliding for broadband gas detection

**Panče Naumov,*[ab] Kenji Sakurai,[c] Akihiko Nukui[a] and Masahiko Tanaka[d]**

*Received (in Cambridge, UK) 31st July 2006, Accepted 24th October 2006*
*First published as an Advance Article on the web 14th November 2006*
**DOI: 10.1039/b610950k**

**A new three-level structural approach based on anion-induced intracolumnar gliding of stacked coordinatively unsaturated units is described for design of metal–organic crystals which exhibit concentration- and gas-specific adsorption of a variety of small molecules and could be employed for multiple and rapid qualitative and quantitative broadband detection of gases or gaseous mixtures.**

Novel materials which are capable of adsorption of gases with rapid and drastic change of their physical properties are important as active components of chemical sensors for detection of harmful air contaminants.[1] A prerequisite for gas adsorption by such materials is high porosity, usually provided by channels or voids in loosely packed inorganic, organic or metal–organic architectures, which are often obtained *via* special synthetic procedures.[2] Here, we suggest a simple crystal engineering strategy for the design of low-cost, efficient and reusable gas-sensing materials for rapid detection of small-molecular gases. Our strategy, exemplified by anion-induced modification of a structure containing the square-planar cation $[Cu(dien)_2]^{2+}$ (dien = *N*,*N*-diethylethylenediamine), utilizes coordinatively active (unsaturated) copper(II) centers which are spaced out by bulky, fairly flexible, asymmetric ligands. Ligands such as dien play a double structural role: the bulky alkyl groups space out the active metal centers and prevent dimerization, while the asymmetric substitution increases the crystal porosity which is a prerequisite for guest diffusion and access of the metal. In the isomorphous triclinic phases of the perchlorate (**1**) and tetrafluoroborate (**2**) salts of $[Cu(dien)_2]^{2+}$, which have been reported previously with respect to their ability for multimode (pressure-, temperature- and light-induced) phase switching,[3] the coordination planes form columnar stacks parallel to the *a*-axis (Fig. 1(a)). Although within the stacks the active copper centers of **1** and **2** are spaced out by void 'pockets' of suitable size for inclusion of small guests ($d$(Cu···Cu) = 8.093(3) Å (**1**) and 8.014(1) Å (**2**) at 295 K), the inter-columnar channels are protruded by oxygen (**1**) and fluorine (**2**) atoms from the anions which prevent diffusion of guests and limit their mobility in the crystal interior. The hindered guest diffusion and mobility results in very low gas susceptibility, so that, for example, if **1** is exposed to non-dried air, no reaction with moisture is observed over months.

[a]*ICYS, National Institute for Materials Science, 1-1 Namiki, Tsukuba, Ibaraki, 305-0044, Japan. E-mail: naumov.pance@nims.go.jp; Fax: +81-29-860-4706; Tel: +81-29-851-3354 8572*
[b]*Institute of Chemistry, Faculty of Science, Sts. Cyril and Methodius University, POB 162, MK-1000, Skopje, Macedonia*
[c]*X-ray Physics Laboratory, Quantum Beam Center, National Institute for Materials Science, 1-2-1 Sengen, Tsukuba, Ibaraki, 305-0047, Japan*
[d]*WEBRAM, SPring-8, National Institute for Materials Science, 1-1-1 Kouto, Mikazuki-cho, Sayo-gun, Hyogo, 679-5198, Japan*

Aimed to enhance the solid-state reactivity, the spherical counter-ions in **1** and **2** were substituted with the planar nitrate. Characterization of the nitrate salt $[Cu(dien)_2](NO_3)_2$ (**3**) with thermal methods, optical microscopy and X-ray diffraction† showed that contrary to the triclinic ($P\bar{1}$) crystals of **1** and **2** which undergo a phase transition without hysteresis around ambient temperature (at 318 K and 303 K, respectively),[3] the monoclinic ($P2_1/n$) symmetry of **3** results in a much higher transition point (376 K) and thermal hysteresis (Fig. 4(b)). The continuous temperature gradient of the ligand-field strength and the phase transition of the crystals of **3** are visually observable as a gradual color change from bright orange below 10 K to dark red around the transition at 376 K (Fig. 2(a)).

In the crystal of **3** (Fig. 1(b)), the coordination planes are glided with respect to each other, which results in an offset of the active void pockets, deshielding of the metal and longer intermetal distance ($d$(Cu···Cu) = 8.186(1) Å at 200 K) relative to **1** and **2**. The increased porosity of **3** is reflected in a lower crystal density (1.45 g cm$^{-3}$, compared to 1.56 g cm$^{-3}$ of **1**). Due to the lowering of the symmetry of the planar $D_{3h}$ nitrate ions relative to the approximately spherical $T_d$ perchlorate and tetrafluoroborate, it was expected that difference in the ion packing might enhance the guest diffusion between the columns of **3** relative to **1** and **2**.

Indeed, when exposed to gaseous $H_2O$, $NH_3$, $H_2S$, $SO_2$ or $NO_x$, powdered or single crystals of **3** exhibit a rapid, gas-specific and drastic color change, monitored as a gradual decrease of the 470 nm absorption band and evolution of new bands whose maxima depend on the adsorbed gas (Fig. 2(b)). The products were characterized by combination of opto–magneto–thermo–structural methods. Reaction with $H_2O$ and $NH_3$ affords well-defined microcrystalline blue powders of **3**·$H_2O$ ($\lambda_{max}$ = 580 nm) and **3**·2$NH_3$ ($\lambda_{max}$ = 430, 660 nm), while $H_2S$ yields dark blue partially reduced product ($\lambda_{max} > 800$ nm; upon prolonged exposure, the crystals turn black due to partial reduction). $SO_2$ ($\lambda_{max}$ = 330, 570 nm) and $NO_x$ ($\lambda_{max}$ = 430, 750 nm) react slowly, affording dark red deliquescent solids. As monitored by the change of the absorption spectra (Fig. 3), for each reacting gas, the diffusion rate, the color intensity and the product yield depend on the reaction time, the gas concentration, the particle size and on the initial treatment of the crystals of **3** after separation from the crystallization solution. Powders or fresh (non-evacuated) single crystals of **3** react instantaneously, while larger single crystals (several millimeters) dried in vacuum react after several minutes. The larger guests $SO_2$ or $NO_x$ react more slowly than the others and the color change is less drastic. The solid–gas reactions are also very sensitive to the concentration of the gas: a difference in relative humidity of 20% during equal exposure time of **3** results in

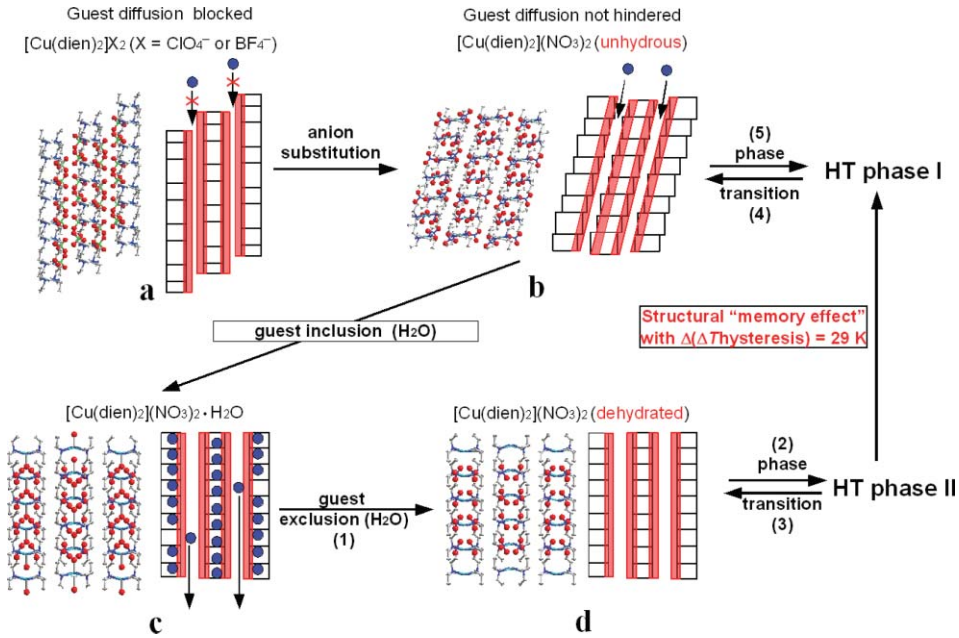


**Fig. 1** Ion packing model and structure schematics of the anion- and guest-induced effects on the structure of the bis(*N*,*N*-diethylethylenediamine)copper(II) salts. 'HT phase I' and 'HT phase II' denote the high-temperature phases of *anhydrous* (initial state, b) and *dehydrated* (after dehydration of the product obtained by exposure to humidity, d) $[Cu(dien)_2](NO_3)_2$ (**3**), respectively. Rectangles and red stripes represent cationic and anionic substructures.

doubled intensity of the 580 nm band of the product **3**·$H_2O$ (Fig. 3(b)). The gas adsorption is reversible, so that crystals of **3**·$H_2O$ and **3**·$2NH_3$ can be repeatedly switched between red and blue by alternative heating (or prolonged evacuation with rotary pump) and exposure to non-dried air or ammonia gas (Fig. 2(c)).

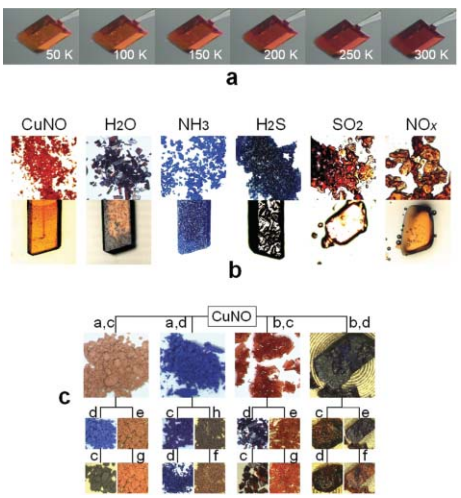


**Fig. 2** Appearance of crystalline **3** (CuNO) treated under various conditions. (a) Thermochromism of a single crystal in a temperature-controlled gas stream due to continuous change of the ligand-field strength. (b) Color change induced by solid-state reaction with various gases. A few seconds after the reaction onset the partially reacted crystal in the case of $H_2O$ shows formation of spatially resolved domains of the reactant and the product. (c) Color change of single crystals and microcrystals upon consecutive thermal, evacuation and humidity treatment: (a) powder, (b) crystalline, (c) vacuum-desiccated, (d) exposed to air, (e) heated to 385 K, (f) heated to 400 K, (g) cooled to 320 K, (h) heated to 340 K.

The possibility for adsorption of gaseous mixtures, which is prospective for 'broadband' gas sensors for simultaneous gas detection, was tested on a mixture of $H_2O$ and $NH_3$, both of which form products of well defined stoichiometry. Reaction of **3** with pure $H_2O_{(g)}$ and $NH_{3(g)}$ yields deep-blue **3**·$H_2O$ and light-blue **3**·$2NH_3$, respectively. Use of $NH_{3(l)}$ instead of $NH_{3(g)}$ affords a blue product, which was characterized by HS/GC-MS, spectroscopic, thermal and powder diffraction methods as a binary mixture **3**·$H_2O$/**3**·$2NH_3$. Dependence of the ratio of adsorbed gases on the concentration of ammonia solution and thus on the partial vapor pressure of the two gases was observed, which paves the way for use of **3** or similar compounds for qualitative and quantitative analysis of gaseous mixtures.

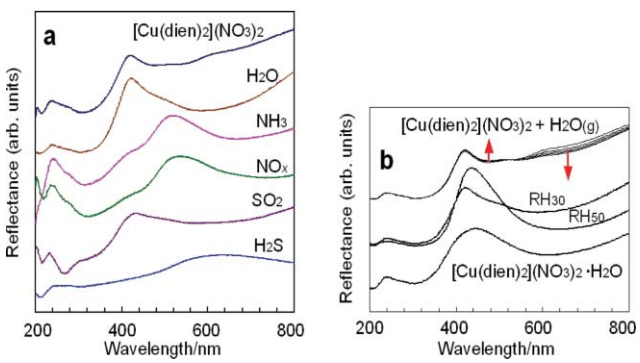


**Fig. 3** (a) Change of the reflectance spectrum of $[Cu(dien)_2](NO_3)_2$ (**3**) upon reaction with various gases. (b) Change of the reflectance spectrum of **3** upon reaction with gaseous $H_2O$. Top: Temporal evolution of the reflectance spectrum of **3**·$H_2O$ obtained from polycrystalline **3** which was exposed to air with traces of constant humidity. The arrows denote the direction of the intensity change. Middle: Change of the reflectance spectra of **3** exposed to relative humidity (RH) of 30% ($RH_{30}$) and 50% ($RH_{30}$) during 5 s. Bottom: Reflectance spectrum of pure **3**·$H_2O$.

 

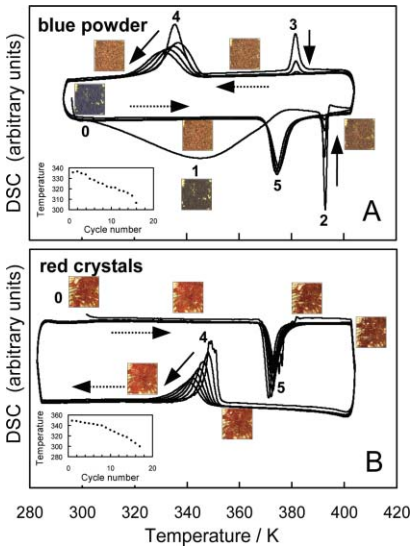


**Fig. 4** Cyclic differential scanning calorimetry (DSC) of $3{\cdot}H_2O$ (blue powder, A) and **3** (red crystals, B). Insets: Dependence of the position of peak (4) on the temperature cycle. Solid and broken arrows show decrease of peak intensity and direction of temperature change, respectively.

The high-resolution powder X-ray diffraction pattern of the microcrystalline product $3{\cdot}H_2O$ (obtained by exposure of **3** to non-dried air), recorded using synchrotron X-ray radiation‡ allowed structure refinement and confirmed the identity of the structure with the single-crystal data.§The water molecules in the pockets of $3{\cdot}H_2O$ occupy the apical position of stacked $CuN_4(OH_2)$ square pyramids (Fig. 1). In the case of ammonia, the spectroscopic data suggest that each pocket in $3{\cdot}2NH_3$ hosts two $NH_3$ molecules which are situated at the axial positions of $CuN_4(NH_3)_2$ octahedra. The cationic substructure of $3{\cdot}H_2O$ (Fig. 1(c)) shows that upon guest inclusion, the offset coordination planes in the *anhydrous* **3** (Fig. 1(b)) have slid back, and in the hydrated crystal $3{\cdot}H_2O$ they are stacked parallel to the *b*-axis in a fashion similar to **1** and **2** (Fig. 1(a)). However, contrary to **1** and **2**, due to the planarity of the nitrate, the intercolumnar channels in $3{\cdot}H_2O$ remain free from the anion oxygen atoms, so that desolvation of $3{\cdot}H_2O$ to *dehydrated* **3** (Fig. 1(d)) is feasible. Accordingly, the DSC curves of heated $3{\cdot}H_2O$ (Fig. 4(a)) show dehydration over a broad temperature range (300–370 K, point (1)). At 393 K, point (2), a portion of the dehydrated **3** is converted to the anhydrous **3**. The creation of binary mixture of phases above point (2) was confirmed by *in situ* temperature-resolved powder diffraction. During the subsequent four thermal cycles, the phase mixture exhibits two phase transitions: the thermochromic transition (4) (335 K)–(5) (374 K) ($\Delta T_{hys,1}$ = 39 K) of the *anhydrous* **3**, and the respective phase transition (2) (393 K)–(3) (383 K) ($\Delta T_{hys,2}$ = 10 K) of the *dehydrated* **3** with partial conversion to the anhydrous **3** (Fig. 4(a)). The occurrence of two simultaneous processes in the case of $3{\cdot}H_2O$ – relaxation of the dehydrated component to the anhydrous one and the thermochromic transition of the latter, is supported by the double-hump appearance of the position profile of peak (4), which is different from the monotonous decrease of the same peak in the case of the DSC curve of the anhydrous **3** (see the insets in Fig. 4). After the conversion dehydrated **3** → anhydrous **3** has been completed in five cycles, the phase transition (2)–(3) vanishes and the DSC profile of $3{\cdot}H_2O$ becomes identical to that of the anhydrous **3** (Fig. 4(b)).

The DSC/X-ray data evidence that hydration of **3**, in which the coordination planes are glided in respect to each other (Fig. 1(b)), and subsequent dehydration of the product $3{\cdot}H_2O$ in which the coordination planes are stacked (Fig. 1(c)), affords a metastable dehydrated phase (Fig. 1(d)) in which the active units are still stacked and which retains 'information' about the structural perturbation induced by the guest water molecules. This structural memory effect can be erased completely by structural relaxation above the high-temperature transition point in five thermal cycles. Collateral sliding of the stacks can be suggested to explain the temperature shift of the high-temperature phase transition of the dehydrated **3** to that of anhydrous **3**. Relative to the anhydrous compound, the latent strain in the structure of the dehydrate results in narrowing of the hysteresis gap of 29 K ($\Delta T_{hys,1} - \Delta T_{hys,2}$) and 19 K increase of the thermochromic transition (peak (5) → peak (2) in Fig. 4(a)).

In summary, here we described a strategy for structural design of inexpensive gas-sensitive crystalline materials, a novel gas-adsorbing material and several solid–gas reactions which exhibit drastic color change. Our strategy is based on design of structures by building up through three levels of structural organization. The *first* level of structural complexity consists of square-planar metal centers with partially saturated coordination spheres and dangling valences that are susceptible for coordination. At the *second* level, these active centers are arranged into columns and spaced out from each other by void pockets which can nest the gas molecules. The *third* level of organization, which is the key point in the construction of this architecture, was introduced as anion-induced off-axis gliding of the adjacent coordination planes to enable fast diffusion of the guest molecules into the pockets. This three-level organization ultimately provides a staircase-like structure of low density and sufficient porosity through which the guests can effectively diffuse into the crystal interior.

We thank Dr T. Fujita and Dr Y. Uemura for their kind help with the experiments, Dr A. A. Belik (magnetic susceptibility) and Dr K. Miura (powder X-ray data). This study was performed through Special Coordination Funds for Promoting Science and Technology from the Ministry of Education, Culture, Sports, Science and Technology of the Japanese Government.

## Notes and references

† CCDC 622953. For crystallographic data in CIF or other electronic format see DOI: 10.1039/b610950k
‡ CCDC 616567. For crystallographic data in CIF or other electronic format see DOI: 10.1039/b610950k
§ CCDC 616566. For crystallographic data in CIF or other electronic format see DOI: 10.1039/b610950k

1 R. B. Vasiliev, L. I. Ryabova, M. N. Rumyantseva and A. M. Gaskov, *Russ. Chem. Rev.*, 2004, **73**, 939.
2 Notable article on crystal porosity: L. J. Barbour, *Chem. Commun.*, 2006, 1163; (*a*) Selected examples of solid-gas reactions: N. Tokitoh, Y. Arai, T. Sasamori, R. Okazaki, S. Nagase, H. Uekusa and Y. Ohashi, *J. Am. Chem. Soc.*, 1998, **120**, 433; (*b*) O. Saied, T. Maris and J. D. Wuest, *J. Am. Chem. Soc.*, 2003, **125**, 14956; (*c*) T. K. Maji, G. Mostafa, R. Matsuda and S. Kitagawa, *J. Am. Chem. Soc.*, 2005, **127**, 17152; (*d*) L. Dobrzanska, G. O. Lloyd, H. G. Raubenheimer and L. J. Barbour, *J. Am. Chem. Soc.*, 2006, **128**, 698.
3 (*a*) A. Nishimori, M. Sorai, E. A. Schmitt and D. A. Hendrickson, *J. Coord. Chem.*, 1996, **37**, 327; (*b*) I. Grenthe, P. Paoletti, M. Sandström and S. Glikberg, *Inorg. Chem.*, 1979, **18**, 2687; (*c*) P. Naumov, K. Sakurai, T. Asaka, A. A. Belik, S. Adachi, J. Takahashi and S. Koshihara, *Chem. Commun.*, 2006, 1491; (*d*) P. Naumov, K. Sakurai, T. Asaka, A. A. Belik, S. Adachi, J. Takahashi and S. Koshihara, *Inorg. Chem.*, 2006, **45**, 5027.